LCC-0081
June 2002
Rev. 2 Dec. 2004

Linear Collider Collaboration Tech Notes

Impact of Surface Preparation on RF Breakdown Performance in NLCTA Accelerating Structures

R. E. Kirby, F. Le Pimpec, F. Marcelja, C. Pearson

Stanford Linear Accelerator Center
Stanford University
Menlo Park, California

Abstract: *In an effort to locate the cause(s) of high electric-field breakdown in X-band accelerating structures, a systematic study was begun on characterizing the effect of etching time on surface roughness, using OFE copper witness coupons made of the same material that was used for structures and machined in identical fashion to those structures. It was found that the minimum surface roughness corresponded to 45 and 5 second etching times on conventional and single=crystal, diamond machined surfaces, respectively. These values are essentially identical, within error, to the times used to obtain the best breakdown results for either type of machined structure.*

Impact of Surface Preparation on RF Breakdown Performance in NLCTA Accelerating Structures

R.E. Kirby, F. Le Pimpec, F. Marcelja, C. Pearson
SLAC, 2575 Sand Hill Road Menlo Park, CA 94025

6th December 2004

Abstract

In an effort to locate the cause(s) of high electric-field breakdown in x-band accelerating structures, a systematic study was begun on characterizing the effect of chemical etching time on surface roughness, using OFE copper witness coupons made of the same material that was used for structures and machined in identical fashion to those structures. It was found that the minimum surface roughness corresponded to 45 and 5 sec etching time on conventionally- and single-crystal diamond-machined surfaces, respectively. These values are essentially identical, within error, to the times used to obtain the best breakdown results for either type of machined structure.

1 Introduction

Next Linear Collider (NLC) accelerating structures, running at 11.424 GHz, are expected to hold a steady operational surface gradient of 73 MV/m, without breakdown arcing.

A development program for the required structure has been in progress at SLAC for several years. Possible rf structure candidates are tested in a specially dedicated linac at SLAC, the Next Linear Collider Test Accelerator (NLCTA). So far, mixed results have been obtained during high electric field-processing of structures. To better understand the differences encountered during the performance of those structures, a materials analysis program has been setup to characterize the surface preparation of the cells constituting the structures. It has been long known that the initial cleanliness of high field structures is key to successful performance, a factor which is not easy to control given the myriad of personnel and procedures involved in producing and installing a finished structure from a billet of raw material [1] [2] [3].

The purpose of this paper is to relate the structures' surface preparation processes to the rf structures' performance during exposure to high electric fields.

2 Causes of Breakdown

Breakdown Sequence: It is known that field emission (FE) is the source of electrons triggering a sequence of events that eventually leads to a breakdown [4] [5]. Electrons,

produced by FE, heat the surface which then releases locally-available gas. Electrons also ionize the gas to form a plasma. Plasma ions are accelerated back toward the now-cathodic surface, releasing more gas. This regenerative mechanism may lead to an enhancement of the plasma density and, eventually, to a breakdown. Therefore, to get a breakdown, it is necessary to provide field emitters and (dissolved) gas.

Emitter Candidates: Dust (carbonaceous fragments,building materials such as concrete, fibers), voids (caused or revealed by etching), grain edges (revealed by chemical etch or furnace thermal-etching), inclusions (usually native to raw material production)and facets (formed by mass movement to lower the local surface free energy).

Dust in our case appears to be introduced into the structure following furnace heating. The dust is stuck to surface electrostatically and by Van der Waals force. Chemical etching is usually required to remove the dust from the surface so its introduction is best avoided by good housekeeping. In-situ, the dust burns off during rf structure-processing, and often carries sufficient dissolved gas for the plasma. The processing-removed dust leaves a residue of carbon (and Si, Al, Mg, Ca, Cl, Ti, etc...typically building-material debris)on the surface, sometimes as a lump.

Voids and Etching Artifacts have not been observed to be a focus of breakdown, probably because they are usually below surface-level. During the furnace cycle, the oxide or etch residue sometimes present in the feature is vaporized. However, the features are not always themselves removed (through mass movement) by the furnace processing.

Grain Edges are often displaced vertically by grain growth (mass movement) in the furnace. The exposed edges are dangerous because of close proximity to dissolved gas in the grain boundary. Displacement is unavoidable but can be minimized by reducing furnace temperature and time.

Inclusions are foreign-material masses lodged in the surface, and are often dielectric (e.g., copper oxide) acting as charged "antennae" with gas often trapped below them. To minimize such these defects, it is necessary to use the highest quality material (OFE Class 1).

Facets appear as copper hillocks. They are small, metallic and good field emitters that can probably sustain healthy FE currents without melting. Keeping the furnace processing time short minimizes the mass movement that produces them. This is especially important on single crystal diamond finish-machined (SCDM) because of its (otherwise) low surface roughness.

3 Experimental Details

The cells constituting the successive NLCTA accelerating structures have been made of several sources of copper. They have also been machined and cleaned differently. To reconstruct and understand what happened to the raw copper material from machining to the creation of an rf structure, a small number of coupon samples of the existing original batches of copper, when available, have been machined, see Figure 1.

Cells for NLCTA structures have been either polycrystalline diamond finish-machined (PCDM), or single crystal diamond finish-machined (SCDM), but principally the first method.

[0] 1"=2.54 cm

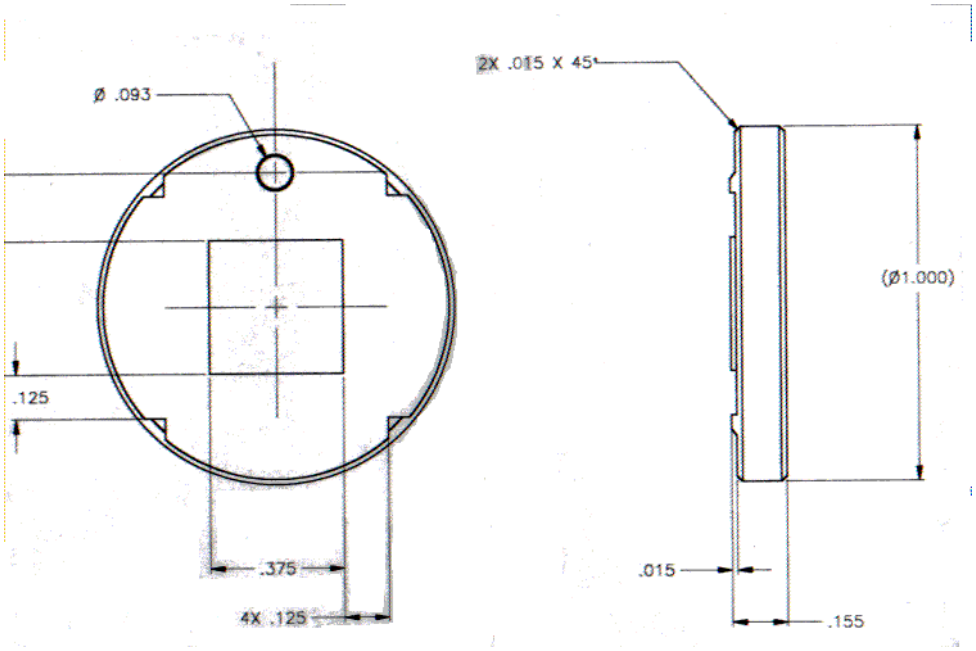

Figure 1: Sample technical drawing (dimensions are in inches)

After stress-relieving the copper to temperatures between 500°C and 525°C, the coupons (as are the cells) are rough-machined (to within a few tenths of a millimeter of finished size), prior to final precision PCD-machining at Robertson, Inc. Some SCDM coupons were prepared at Lawrence Livermore Lab (LLNL) where the procedure prior to SCD-machining is the same as PCDM. Final SCD-machining was done with ethanol as the machining fluid. Other SCDM coupons were prepared at KEK (Japan). Stock was vacuum-annealed at 500°C for 1 hour, thenSCD-turned using Kerosene. Coupons were then degreased with alcohol and acetone. The finished coupons from LLNL and Robertson are perchloroethylene-degreased, KEK coupons were measured as-received, and then submitted to a battery of tests. These included micro-balance weighing and measurement by x-ray photo-electron spectroscopy (XPS) to look at the baseline of contaminants present on the as-machined and degreased surface. The average roughness of the surface was measured by atomic force microscopy (AFM) and by a profilometer. The topography of surface and near-surface features features are revealed using a secondary electron microscope (SEM) and backscattered electron microscopy (BSE). Finally, in some cases, an optical microscopic picture of the surface was also taken.

Schematics of the analyzing tools can be found in [6]. The energy of the electron, impinging the surface at normal incidence, used for the SEM and BSE analyses is 15 keV. The secondary electrons have an escape depth of 1-2 nm, while the BSE electrons probe the sub-surface up to 500 nm depth [7].

PCDM coupons were etched for 5, 30, 60,and 120 seconds each and the SCDM coupons for 0, 5, 30, and 60 seconds. The unetched coupon acted as an as-machined witness. The etching solution was composed of 70% phosphoric acid, 23% of nitric acid, 6.7% of acetic acid and the remainder hydrochloric acid. After etching, the coupons followed the NLCTA cell-processing schedule, simulated below.
The cells composing the structure are kept inside a clean alcohol-filled container until

blow-dried with filtered dry nitrogen gas, for delivery to diffusion-bonding and brazing. Our coupons have followed the same procedure, but before delivering them for furnace-heating, a second set of surface analyses was performed.
Finally, the coupons were heat-treated in a dry-hydrogen for two hours at 1020°C and four hours at 950°C to simulate the diffusion bonding, brazing and vacuum-baking processes. The total time in hydrogen atmosphere is still less than that experienced by an actual structure, but we do believe that after a few hours at a temperature of about 1000°C, the copper mass movement is essentially completed. Following this heat treatment, a final set of surface analyses were completed on the samples.

4 Results and Discussion

The first action of chemical etching is to remove material from the surface. Figure 2 shows the evolution of the thickness removed versus the etching time in the acid-etching bath. We have to keep in mind that only 1 cm^2 of the coupon has received the finish-machine treatment. So most of the mass is removed from the roughest part of the sample. The acid may not be as aggressive at removing material on the high quality finished area on top of the mesa, cf. Figure 1. Despite this unknown, a thirty-second etch is already sufficient to remove some particles from the surface as shown in Figure 3. The black spot on the far left side of the picture may be a void or a low-density particle. Comparison of SEM and BSE images allow us to differentiate between the two possibilities, Figure 4 and Figure 5.

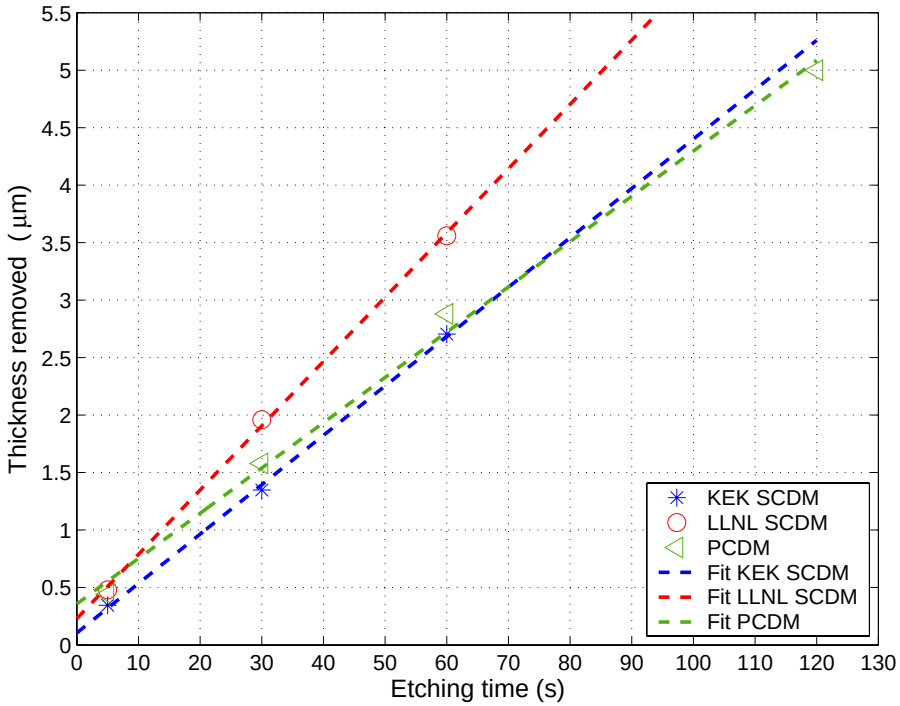

Figure 2: Microbalance-weighing results after etching the coupons

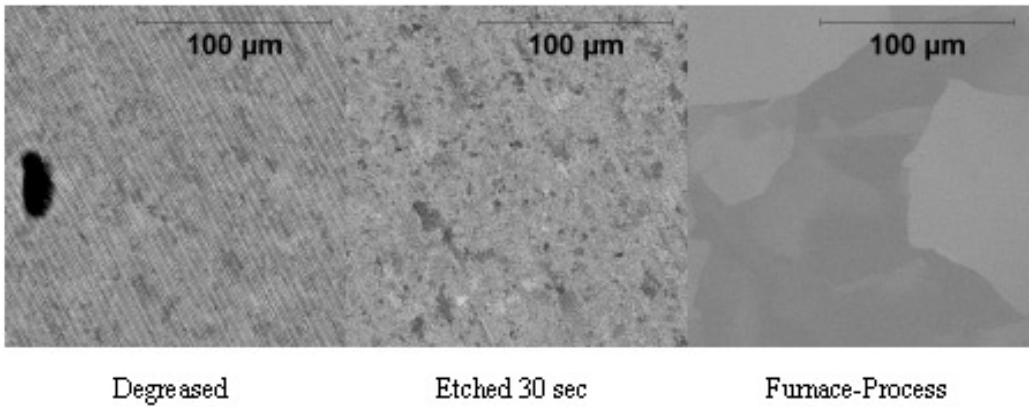

Figure 3: BSE picture of a PCDM coupon after each step of processing

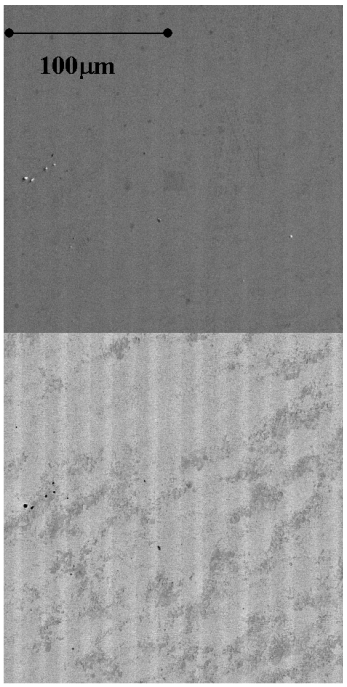

Figure 4: SEM (top) and BSE (bottom) pictures of a (LLNL) SCDM mesa before etch

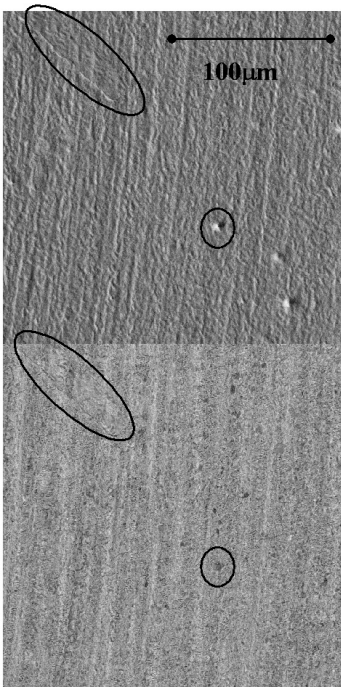

Figure 5: SEM (top) and BSE (bottom) pictures of a PCDM mesa after a 60 s etch

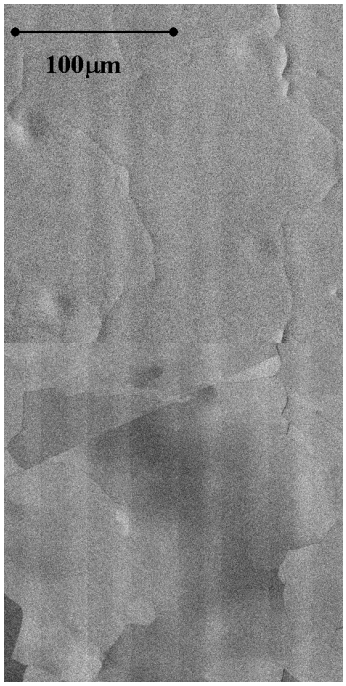

Figure 6: SEM (top) and BSE (bottom) pictures of a PCDM mesa after the 60 s etch and hydrogen furnace cycle

The action of subsequent etching does not remove systematically the same thickness, Figure 7. All the damages seem to be produced in the first 60 s of the etch. The thickness removed for the PCDM sample, etch for 2 minutes, Figure 2, is almost equivalent of the thickness removed by two cycles of 1 minute etch.

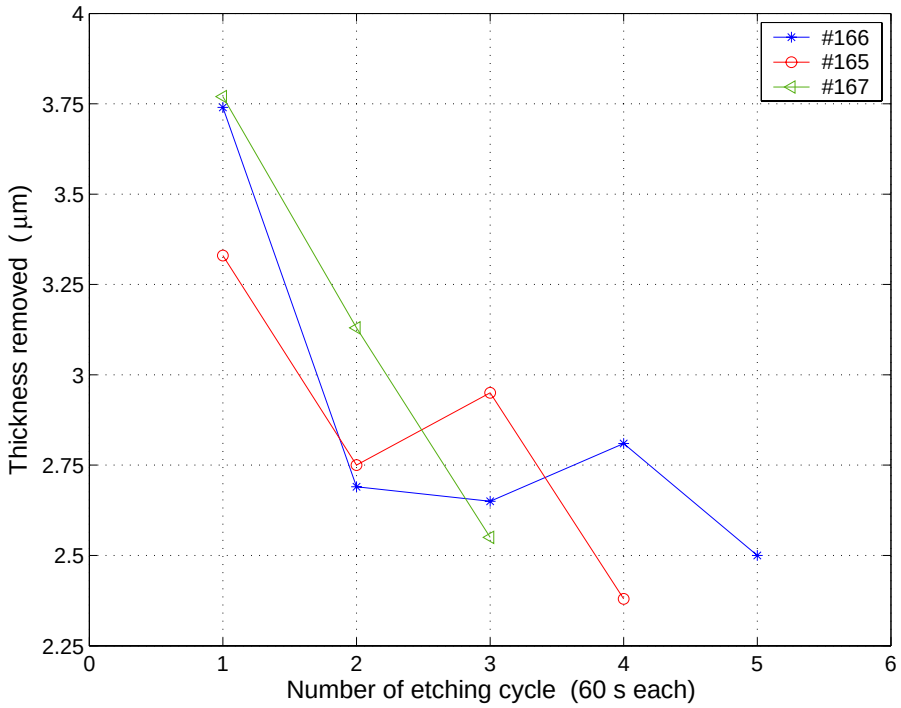

Figure 7: Microbalance-weighing results after 60s etching cycle on PCDM sample non-stress relieved. Most of the damage layer is rapidly removed in the first 1.5 μm of surface.

In addition to removing copper material and particles, the second action of etching is to alter the surface roughness. It is known that the metal etch rate is sensitive to lattice crystal orientation [8] and, possibly, machining-induced stess. This contention is evident from comparing the average roughness of the mesa surface between PCDM and SCDM coupons.

The roughness has been measured by two different apparatus. The area scanned by the AFM tip is typically a rectangle of $\sim$ 50x70 μm. This size is smaller than the average grain size of the copper sample. The profilometer measures the roughness along a line of 3 mm from the center line up of the mesa of the sample 1 and 3 mm from the center line down. The results obtained using Equation (1), average roughness, are presented in Tables 1, 3 and 5 for the AFM scan, and summarized in Tables 2, 4 and 6 for the profilometer.

$$R_a = \frac{1}{N} \sum_{1}^{N} |Z_i - Z_{avrg}| \tag{1}$$

where N is the number of samples ($\sim$ 4.2 10^6), and Z is the height. The zero is taken for the lowest Z measured by the AFM.

Roughness surface analysis of the results obtained by the AFM is obtained by doing multiple cross section of the area scanned, avoiding obvious etch pit or hillocks, or taking an average of the R_a from a define area. We did not systematically use the R_a from the full area provided by the AFM software as it tends to be equal or greater, up to a factor 2, than the careful manual analysis. The reason is that surfaces which have a bow in an axis direction will see a maximum peak to lower peak value higher than the peak to peak without the bow. Also for our AFM, very flat surfaces as the SCDM, presents artificial lines, which can contribute to skew the data. However, for the etched surfaces, the R_a from the full area provided by the AFM software is greater by $\sim 22\%$. Results obtain by the profilometer is also dependant of the profile scanned. It is important to do the measurement on places which at the naked eyes looked average for the sample avoiding obvious scratches and pits. On smooth surfaces a peak due to a dust can skew the R_a by a factor 2 or even more.

Coupon #	143	144	145	146
Bare machining (nm)	128.7	100.6	123.9	130
After Etching (nm)	105.1 (5")	40.4 (30")	44.4 (60")	90.5 (120")
Heat treatment (nm)	67.1	35.6	31.3	53.1

Table 1: Polycrystalline diamond-machined, average roughness measured with an AFM

Coupon #	143	144	145	146
Heat treatment Top (nm)	58.4	82.9	63.2	106.9
Heat treatment Bottom (nm)	59.9	72.7	73.6	123.9

Table 2: Polycrystalline diamond-machined, average roughness measured with a profilometer over two half side of the mesa sample Fig.1

Coupon #	137	138	139	140
Bare machining (nm)	4.7	6.3	8.7	3.3
After Etching (nm)	4.7 (0")	6.3 (5")	12.5 (30")	21.3 (60")
Heat treatment (nm)	-	8.0	19.9	20.6

Table 3: LLNL Single crystal diamond-machined, average roughness measured with an AFM

A direct interpretation of these is that the etching tends to smooth out the surface of a PCDM mesa and roughen the surface of a SCDM mesa. The high-temperature treatment of these samples in the hydrogen furnace also gives also different results, depending on the nature of the machining finish. Heat treatment smoothes the PCDM mesas, Figures 5 and 6, and roughens the SCDM mesas.
Also the movement in the grains creates hillocks which are visible, with AFM, on SCDM surfaces [9]. These hillocks are probably too small, at less than 100 nm, to contribute significant FE current. However, they may contribute to the overall enhancement of the

Coupon #	137	138	139	140
Heat treatment Top (nm)	4.6	14.1	45.8	28.3
Heat treatment Bottom (nm)	13.4	16.8	24.5	35.8

Table 4: LLNL Single crystal diamond-machined, average roughness measured with a profilometer over two half side of the mesa sample Fig.1

Coupon #	KEK 1	KEK 2	KEK 3	KEK 4	KEK 5
Bare machining (nm)	7.3	6.1	7.3	8.1	8.1
After Etching (nm)	13.6 (5")	12.3 (0")	19.9 (30")	33.4(60")	- (0")
Heat treatment (nm)	13.6	12.4	17.6	52.6	-

Table 5: KEK Single crystal diamond-machined, average roughness measured with an AFM

Coupon #	KEK 1	KEK 2	KEK 3	KEK 4	KEK 5
Bare machining Top (nm)	17.5	30.4	22.2	14.2	17.8
Bare machining Bottom (nm)	27.0	22.8	15.0	13.6	16.4
After Etching Top (nm)	16.3 (5")	29.3 (0")	33.3 (30")	59.1 (60")	19.0 (0")
After Etching Bottom (nm)	16.1 (5")	24.1 (0")	29.1 (30")	52.2 (60")	23.2 (0")
Heat treatment Top(nm)	19.4	19.5	28.9	63.2	-
Heat treatment Bottom (nm)	20.0	17.0	28.2	50.9	-

Table 6: KEK Single crystal diamond-machined, average roughness measured with a profilometer over two half side of the mesa sample Fig.1

field, or participate with other field emitters to the breakdown process.
Optical microscopy performed on PCDM or SCDM coupons reveals that, for a PCDM surface, grain edges are developing after 30 or 60 seconds of etching [9] [10]. The same analysis on SCDM surfaces reveals voids after a 5 s etch and grain edge development at 30 sec, cf. Figure 8 to Figure 10.
The furnace processing of all coupons creates new surface and sub-surface features, as shown in Figure 3 (far right), and Figure 6. The growth of the copper grains is also put in evidence Figure 4

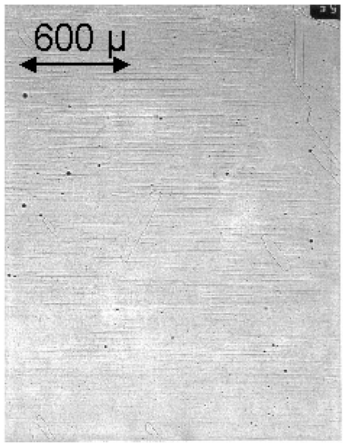

Figure 8: Optical micrograph of a SCDM surface after a 5 s etch

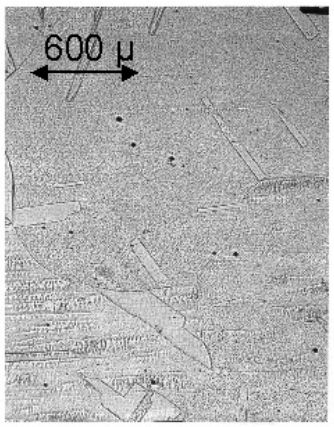

Figure 9: Optical micrgraph of a SCDM surface after a 30 s etch

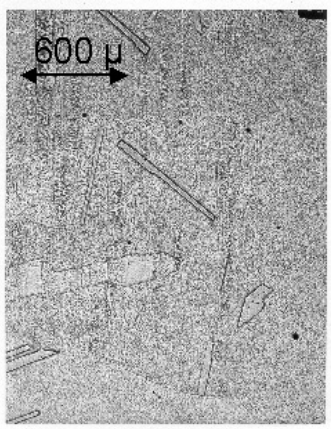

Figure 10: Optical micrograph of a SCDM surface after a 60 s etch

The XPS analysis, of a 4x4 mm^2, shows that the degreased sample, Figure 12, is suitable for use in an UHV (Ultra High Vacuum) environment. A five-second chemical etch is sufficient to reduce the level of carbon further, Figure 13. The analysis, after heat treatment, shows no re-contamination and displays a level of carbon similar to the one obtained after etching. These results are also true for the PCDM samples [9] [10].

If the manufacturing and handling steps for a structure reproduce the controlled steps executed on these test coupons, then extrinsic sources (debris, machining defects) of FE are mostly eliminated. In order to keep this well-prepared surface, it is very important to minimize the number of opportunities for contamination in the assembly and beam-line installation steps. Intrinsic sources can be controlled by the use of the best quality copper for the fabrication of the structure. This will reduce the numbers of impurity inclusions and unconsolidated grains.
In order to prevent raised grain edges and facetting (hillock growth), one has to minimize the etch time and the time spent at elevated temperature. This is especially important in the case of the SCDM structure, since any etching or furnace processing roughens the surface.

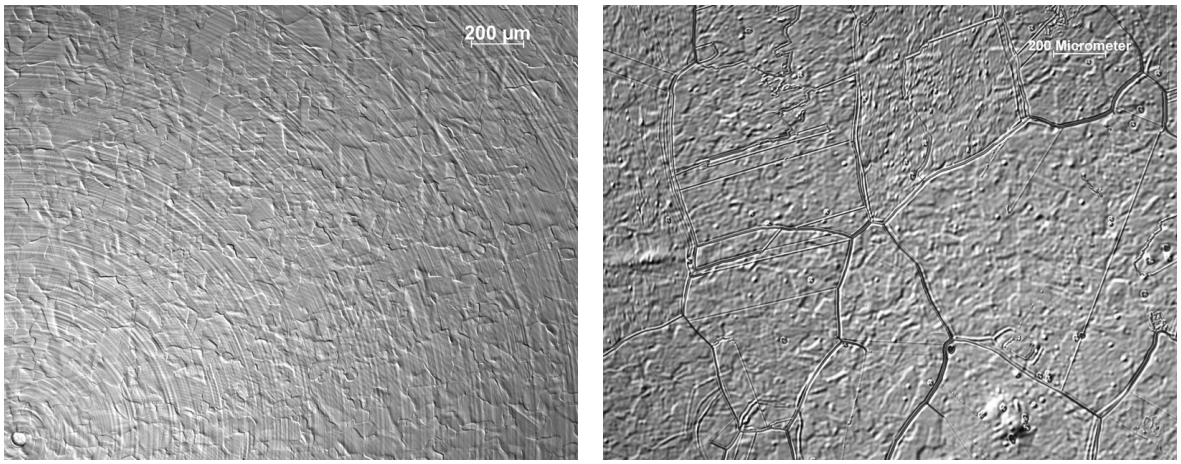

Figure 11: Optical image of SCDM KEK#3 after 30" etch (left) and after the firing cycle (right)

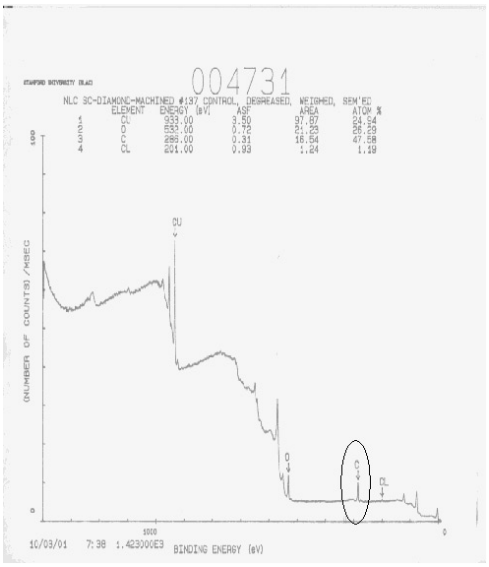

Figure 12: XPS analysis of a SCDM surface before chemical etching.

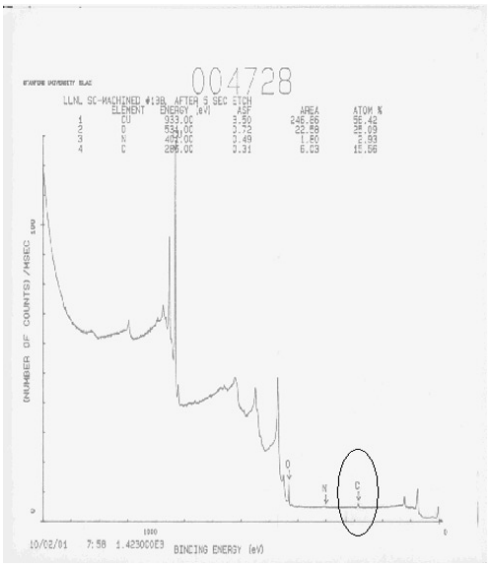

Figure 13: XPS analysis of a SCDM surface after a 5 s chemical etch.

5 Conclusion

Following our extensive research, we came to the conclusion that a 5 s (SCDM) and 30 s (PCDM) etching is sufficient to remove machining lines. To remove sub-surface damage, 30 and 60 s are better but surface grain relief begins to develop. A compromise is to etch SCDM cells for 5 s and PCDM cells for 45 s.

Looking at the results obtained so far, from actual NLCTA structures which have been rf-processed Figure 14, it is clear that the care being taken has allowed the structures to reach the gradient of 73 MV/m required by the design of the future NLC. It is, nevertheless, not sufficient to explain the variation in high-field performance observed among structures manufactured, processed and rf-tested in essentially identical manner.

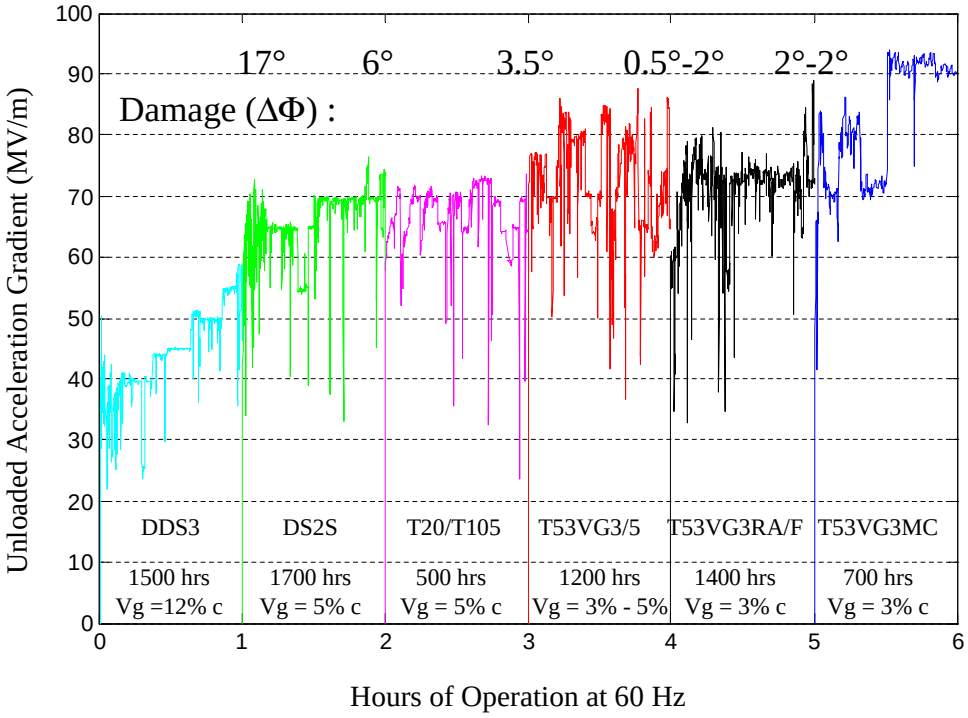

Figure 14: Operation History of nine test structure [11]

6 Acknowledgments

We would like to thank LLNL and KEK for providing single crystal diamond machined samples.

References

[1] C. Suzuki et Al. Fabrication of ultra-clean copper surface to minimize field emission dark currents. *Nuclear Instruments and Methods in Physics Research A*, 462:337, 2001.

[2] S. Kobayashi,Y. Hashimoto, M. Maeyama, Y. Saito and Y. Nagai. Electrical Breakdown Strength of Oxygen-free Copper Electrodes under Surface and Bulk Treatment Conditions. *Vacuum*, 47 (6-8):745, 1996.

[3] J. Tan. *Etude de L'émission Electronique par Effet de Champ en Haute Fréquences*. PhD thesis, Université Pierre et Marie Curie Paris 6, 1995.

[4] J. Knobloch. *Advanced Thermometry Studies of Superconducting RF Cavities*. PhD thesis, Cornell University, 1997. http://w4.lns.cornell.edu /public/CESR/SRF/dissertations/knobloch/knobloch.html.

[5] K. Ohira, A. Iwai, S. Kobayashi and Y. Saito. Parameters Influencing Breakdown Characteristics of Vacuum Gaps during Spark Conditioning. *IEEE Transactions on Dielectrics and Electrical Insulation*, 6 (4):455, 1999.

[6] R.E. Kirby and F. Marcelja. DS2 Structure Autopsy. Technical report, SLAC-NLCTA-066, 2001. http://www-project.slac.stanford.edu/lc/local/notes/rf_process/PDF/DS2StructureAutopsyc.pdf.

[7] H. Seiler. Secondary Electron Emission in the Scanning Electron Microscope. *Journal of Applied Physics*, 54 (11):R1, 1983.

[8] Herbert H. Uhlig, editor. *The Corrosion Handbook*. 9^{th} printing. J. Wiley & Sons, 1966.

[9] R. Kirby, F. Marcelja, F. Le Pimpec, C. Pearson. How Long to Etch the Next Structure? http://www-project.slac.stanford.edu/lc/local/notes/rf_process/PDF/NLCTAEtchDecision_final.pdf .

[10] R. Kirby, F. Marcelja, F. Le Pimpec, C. Pearson. Surface Studies of Breakdown Sites in X-Band Strucutures. In *LC02 Workshop SLAC 2002*, 2002. http://www-conf.slac.stanford.edu/lc02/wg2/session_5.htm.

[11] C. Adolphsen et al. High Gradient Accelerator Structure R&D for the NLC. In *LC02 Workshop SLAC 2002*. http://www-conf.slac.stanford.edu/lc02/wg2/WG2_Adolphsen.pdf.